Cooling cycles in superconductors calculated by dynamical London theory

W. D. Bauer * May 4 2024

Abstract

The classical London theory is extended in order to predict the time-dependent behavior of superconductors. Different to prior models it contains a 2-fold time derivative of the magnetic field B and includes the self induction of the superconducting probe. It predicts an inverted (gain)-hysteresis in the M-H diagram for non-stationary cycles which violates the 2nd law. The gain estimated is measurable.

1 Introduction

The 2nd law exists in different versions which can have different consequences [1]. A generally valid version cannot be found elaborated in the literature so far. So it is believed generally that the 2nd law has to be formulated as principle of maximum entropy.
Substantiated doubts about its general validity exist since the discovery of inverted hysteresis of (relative pure) capacitive and inductive elements. Aharoni [2] mentioned first 1994 that these observations are a hint on a 2nd law violation because inverted electric (or magnetic) (gain-)cycles are proceeded at only one heat bath temperature. A literature research [3] reviews the best candidates. For the most candidate systems the claims are insufficient because a direct energy measurement is missing almost always.
The work of Santhanan et al. [4] describes an overunity effect: Here the light energy emission of an IR-diode is higher than the input energy of the small exciting forward current. Obviously the heat energy of the thermal environment (135^oC) adds to the light emission. This may be caused by phonon-assisted emission [5] [6] . This effect can be found also in the inverted hysteresis of a quantum dot FET capacitance [3] [5].

*email: w.d.bauer@t-online.de

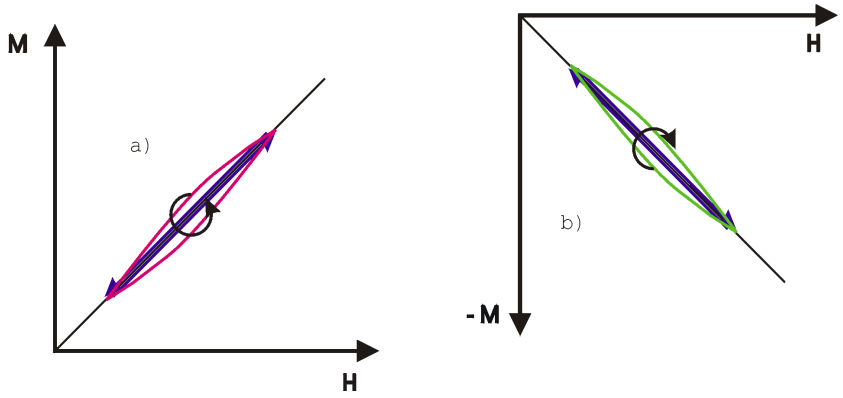

Figure 1: a) M-H - diagram of a para- or ferromagnetic material in a periodic magnetic field. black lines: quasi-stable thermodynamic path, red line: non-stationary loss cycle The orientation of the cycle indicates a loss .
b) M-H - diagram of a diamagnetic or superconducting material in a periodic magnetic field. black lines: quasi-stable thermodynamic path, green line: non-stationary gain cycle The orientation of the cycle indicates a gain .

2 Dynamic London Theory

2.1 Model

2.1.1 motivation

If a para- or ferromagnetic material is subjected to a homogeneous periodical magnetic field H at constant temperature T it shows a loss of magnetic energy described by a loss angle. Qualitatively this can be understood by the principle of causality: The build-up of the magnetization M follows the induction field H with retardation. The loss of magnetic energy during a period is represented by the orientation of the cycle in the corresponding M-H - diagram Fig.1a.
If the same cycle is performed with diamagnetic or superconducting material with the same loss mechanism, the orientation of cycle is reversed indicating an "inverted hysteresis", see Fig.1b. Then, due to energy conservation it holds $-\oint MdH + T\oint ds = 0$ with $-\oint MdH > 0$ and $\oint ds < 0$ (s:=entropy per volume) which violates the 2nd law.
Therefore a dynamical London theory of superconductivity was worked out in order to estimate the gain or loss obtained quantitatively.

2.1.2 the model assumptions

The probe is chosen to have cylindrical geometry and infinite length. The material of the probe is the type-I superconductor lead. The temperature is $T = 4,2K$. The exciting magnetic field $B_0(t)$ is homogenous and in axial direction. The exciting waveform alternates between rising and falling exponential pulses with the time constant ΔT. The material consists of two phases: the superconducting and the resistive phase, see Fig.2. Voltage and current density j_R is generated in the resistive phase and is driven by the time-changing inductive magnetic field dB/dt. It can be shorted by the surrounding superconductor, cf. fig 2. It holds $j_R = \Delta j_S$ at the contact areas. The electrons of the resistive current obey a damped equation of motion.
This allows to develop a time-dependent London differential equation. The homogeneous superconducting part is extended for time-dependency, an inhomogeneous part adds the contribution of the local resistive electron current density $j_R(r)$ driven by the time-dependent inductive magnetic field.

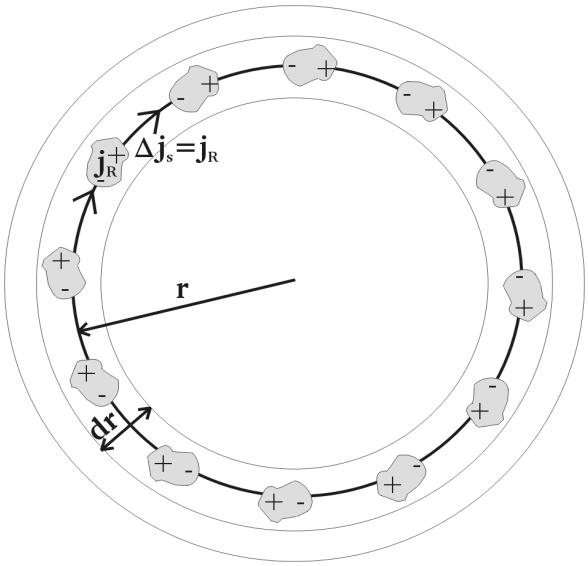

Figure 2: Two-phase model of a type I superconductor
Voltage is generated in the resistive phase by induction and is shorted by the superconducting phase. The current densities at the contact areas are $j_R = \Delta j_S$.

2.1.3 the superconducting phase

The London equation [7] [8] is

$$\mathbf{j} = \frac{-\mathbf{A}}{\mu_0 \lambda_L^2} \tag{1}$$

with $\mathbf{A}$:= magnetic vector potential, μ_0 := induction constant and λ_L := London penetration depth. Therefrom follows

$$\nabla \times \ \mathbf{j} = \frac{-\mathbf{B}}{\mu_0 \lambda_L^2} \tag{2}$$

The dynamical Ampere-Maxwell equation multiplied by μ_0 is

$$\nabla \times \ \mathbf{B} = \mu_0(\mathbf{j} + \frac{d\mathbf{D}}{dt}) \tag{3}$$

with E := electric field and $D := \epsilon_0 E$ dielectric displacement field.
Applying the rot operator follows

$$\nabla \times \nabla \times \mathbf{B} = \mu_0(\nabla \times \ \mathbf{j} + \epsilon\epsilon_0 \frac{d}{dt}(\nabla \times \ \mathbf{E})) \tag{4}$$

with ϵ_0 := dielectric vacuum constant and ϵ := dielectric material constant. After inserting the Faraday-Maxwell law $\nabla \times E = -dB/dt$ one obtains with eq.(2) after some calculations

$$\nabla^2 \mathbf{B} = \frac{\mathbf{B}}{\lambda_L^2} + \mu_0 \epsilon_0 \epsilon \frac{d^2\mathbf{B}}{dt^2} \tag{5}$$

This is the dynamical differential equation of the superconducting phase.
If the last term is omitted it is identical to the stationary London differential equation.

2.1.4 the resistive phase

Generally in a superconducting material it holds for moving charge particles [8] (with m :=mass, v :=velocity, q := charge, p := impulse)

$$p = mv + qA \tag{6}$$

For a stationary superconductor it holds for the impulse $p = 0$.
To extend eq.(6) and change mv to a macroscopic current density j, the contributions of the many single resistive and superconducting charges have

to be summed up. With $n_{R/S}$:= number of resistive/superconducting charges per volume the result can be written

$$j = n_R q_R v_R - \frac{n_S q_S^2}{m_S} A \tag{7}$$

The terms on the right side can be defined as $j_R := n_R q_R v_R$ and $j_S := -A/(\mu_0 \lambda_L^2)$ with $\lambda_L^2 := m_S/(\mu_0 n_S q_S^2)$. Applying the rot-operator to eq.(7) above and multiplicating with μ_0 yields with eq.(1)

$$\mu_0 \nabla \times j = \mu_0 n_R q_R \nabla \times v_R - \frac{B}{\lambda_L^2} \tag{8}$$

If eq.(8) is inserted into eq.(4) we can obtain finally the full inhomogeneous London differential equation, cf. eq. (19).
Here, in order to determine the system completely we solve the equation of motion for the velocity $v(r)$ of the resistive electrons in the superconductor at each radius r of the cylinder or ring

$$m.\frac{dv}{dt} + \gamma.v = F_{ind} + F_{self} \tag{9}$$

$\gamma = n_R q^2/\sigma$ is the friction constant with $\sigma :=$ conductivity.
γ is derived from the equations $F_{el} = \gamma v$, $F_{el} = qE$, $j = \sigma E$ and $j = n_R q v$.
j and E is eliminated and the coefficients of the force equations are compared.
$F_{ind} := q.E_{ind}$ is the force induced by the time-dependent field $B(t)$.
It is derived from Faraday's law (with $r :=$ radius)

$$\oint E_{ind} ds = -\int 2\pi r \dot{B}(r) dr \tag{10}$$

The solution is

$$F_{ind}(r) = -\frac{q}{r} \int_0^r \dot{B}(r) r dr \tag{11}$$

$F_{self} := q.E_{self}$ is the force due to selfinduction. It is derived from the Faraday-Maxwell law

$$\oint E_{self} ds = -\int_0^r 2\pi r \dot{B}_{self}(r) dr \tag{12}$$

$\dot{B}_{self}$ is obtained from Ampere's law $\nabla \times B_{self} = \mu_0.j$ which has to be differentiated for time

$$\oint \dot{B}_{self} ds = 2\pi \int_{x_0}^r \mu_0 q n_R \dot{v}(r) r dr \tag{13}$$

Evaluating eq.(13) for $\dot{B}_{self}$, inserting it in eq.(12) and evaluating eq.(12) for E_{self} the final result $F_{self} := q.E_{self}$ can be written

$$F_{self}(r) = -\frac{q^2 \mu_0 n_R}{r} \frac{d}{dt} \int_0^r (\int_{x_0}^{r'} v(r) r dr) dr' \tag{14}$$

So inserting eq.(11) and eq.(14) in eq,(9) we obtain the time-dependent differential equation with the definition $v_m := v(r).r$

$$m.\dot{v}_m(r) + \gamma v_m(r) = -q \int_0^r \dot{B}(r') r' dr' - q^2 \mu_0 n_R \int_0^r (\int_{x_0}^{r'} \dot{v}_m(r) dr)\ dr' \tag{15}$$

We define as $\Phi :=$ the net magnetic flux/(2 π)

$$\Phi(r) := \int_0^r\ B(r') r' + q\mu_0 n_R (\int_{x_0}^{r'} v_m(r) dr\ )\ dr' \tag{16}$$

and for the following

$$\phi(r') := \int_{x_0}^{r'} v_m(r) dr \tag{17}$$

The solution of the differential equation eq.(15) is (with $\tau := m/\gamma$)

$$v_m(r) := -\frac{q}{m}\ exp(-t/\tau) \int_0^{t_{end}} exp(t/\tau) \dot{\Phi}(r)\ dt \tag{18}$$

2.1.5 the complete differential equation system

The inhomogeneous London differential equation can be derived as mentioned in the last section, cf. eq.(8).
The superconducting part, cf. eq.(5), has also to be expressed in cylindrical coordinates. With the relation $|\nabla \times v| = 2\omega = 2v/r$, see [10] , the equation is

$$\frac{d^2 B}{dr^2} = \frac{B}{\lambda_L^2} - \frac{1}{r}\frac{dB}{dr} + \mu_0 \epsilon_0 \epsilon \frac{d^2 B}{dt^2} - 2\mu_0 n_R q_R v(r)/r \tag{19}$$

Two equations complete the differential equation system, they are (cf. eq.(16))

$$\frac{d}{dr}\Phi(r) = rB(r) + q\mu_0 n_R \phi(r) \tag{20}$$

and cf. eq.(17)

$$\frac{d}{dr}\phi(r) = v_m(r) \tag{21}$$

Sometimes it is recommended to enlarge this system for control or to avoid numerical problems by the code. The additional equation is the difference of the time-dependent minus the stationary London differential equation.
Defining $\delta B := B - B_s$ with $B_s :=$ stationary solution, this equation is

$$\frac{d^2\delta B}{dr^2} = \frac{\delta B}{\lambda_L^2} - \frac{1}{r}\frac{d\delta B}{dr} + \mu_0\epsilon_0\epsilon\frac{d^2B}{dt^2} - 2\mu_0 n_R q v(r)/r \tag{22}$$

If the algorithm is programmed without selfinduction only eq.(19) and eq.(20) (with $\phi = 0$) are needed. The stationary solution needs only eq.(19) and skips all time dependent terms.

3 Results

Fig.3a show the profiles of the magnetic field $B(r)$ and $(B - B_S)(r)$ of a cylinder shortly after an exponential magnetic field $B_0(t)$ is switched on (see figures and appendix for details). Fig.3b shows the same for a ring. Because the deviations $\Delta M(r) := (B - B_S)(r)$ from equilibrium state are small we investigated what happens if the system is subjected permanently to an alternating field $B_0(t)$. Then the energies are summed up which are exchanged between heat and the magnetic field .
This is shown in Fig.4a and Fig.4b.
The $\Delta\bar{M} - H$ - diagram is generated as follows:
At every moment t the radial profile of the probe is calculated. This allows to determine the deviation $B(r) - B_S(r)$ from equilibrium. Therefrom the non-equilibrium change of permeabilty $\Delta\mu(r)$ is calculated according to

$$\frac{B - B_S}{B_0} = \frac{\mu_0(1+\mu)H - \mu_0(1+\mu_S)H}{\mu_0 H} := \Delta\mu(r) \tag{23}$$

This allows to calculate the local non-equilibrium magnetization change $\Delta M(r) := \Delta\mu(r)H$ at r and t_i with $H := B_0(t)/\mu_0$. Therefrom it follows the mean non-equilibrium magnetization change of the probe.

$$\Delta\bar{M} = \frac{2}{r_0^2 - x_0^2}\int_{x_0}^{r_0} \Delta M(r) r dr \tag{24}$$

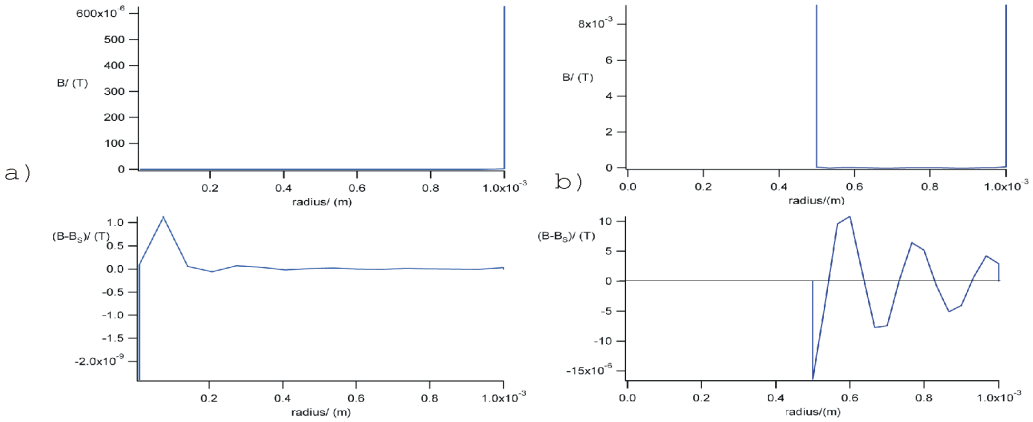

Figure 3:
a) upper diagram: B-r - profile of the cylinder after starting a exponential pulse
lower diagram: $(B - B_S) - r$ - profile
data: $\Delta T = 10^{-7}$s, resolution $80p/\Delta T$, 6 equations, (p:=points)
b) upper diagram: B-r - profile of the ring after starting a exponential pulse
lower diagram: $(B - B_S) - r$ - profile
parameter: $\Delta T = 10^{-7}$s, resolution $10p/\Delta T$, 4 equations

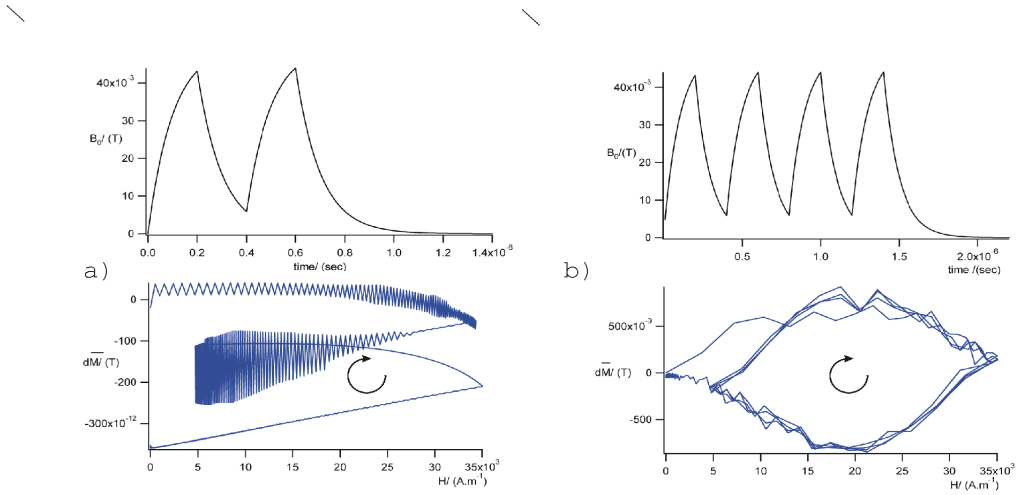

Figure 4:
a) cycling a cylinder: upper diagram: exciting field B_0 vs. time t
lower diagram: non-stationary gain cycle: $d\bar{M} - H$ - diagram
parameter: $\Delta T = 10^{-7}$s, resolution $80p/\Delta T$, 6 eqns., cooling time for 1 °K: $\approx$ 7808s
b) cycling a ring: upper diagram: exciting field B_0 vs. time t
lower diagram: non-stationary gain cycle: $d\bar{M} - H$ - diagram
parameter: $\Delta T = 10^{-7}$s, resolution $10p/\Delta T$, 4 eqns., cooling time for 1 °K: $\approx$ 2.2s

This allows to calculate the magnetic field energy change after a closed cycle

$$\Delta E = \oint \Delta \bar{M} dH \tag{25}$$

The simulation shows that both cycles with the cylinder or the ring yield a gain. The gain of the ring is larger. The result for the cylinder is preliminary and needs further evaluation. If the a cycle is calculated without self-induction, this cycle yields a loss (Fig.5).
Because the field energy is exchanged with heat, a corresponding temperature change per time can be estimated from the specific heat data. The specific heat is a modified T^3-law [12], (material data cf. Tab.1 of appendix)

$$C_P = c_1 (T/T_D)^3 + c_2 T \tag{26}$$

We change this into a heat capacity per volume: (data cf.Tab.1 of appendix)

$$C_{P\_Vol} := 4,186.10^3 \; C_P/(M_{Pb} \; d_{Pb}) \tag{27}$$

From any cycle we obtain the field energy change $\Delta E/\Delta t$ per volume (in dm^3) and time (in sec)

$$\Delta E/\Delta t \approx n \Delta E \tag{28}$$

n is the number of cycles per sec.
Therefrom we obtain the time estimation for cooling the material in the field

$$t \approx \frac{C_{P\_Vol}}{\Delta E/\Delta t}. \tag{29}$$

For numerical results, see Fig.4–6. Numerical data for boundary conditions and geometry can be found in the appendix.
The effects depend also strongly on ΔT (or frequency), see Fig.6a and 6b.
We summarize: The estimations show that the cooling effects are measurable.

4 Discussion

Equilibrium thermodynamics can be regarded to be a stable attractor in the framework of nonlinear dynamics [18]. For a dynamical system $\mathbf{f}(\mathbf{w}, \mathbf{q}; \mathbf{t})$ relaxing to the stationary state of inner energy U, the dependent variables can be interpreted as $\mathbf{w} := (p, T, B)$ and the control parameters as $\mathbf{q} := (V, S, H)$. The mathematical dynamical solution can contradict the 2nd law, if it is an inconsistent additional assumption in the context of the model.

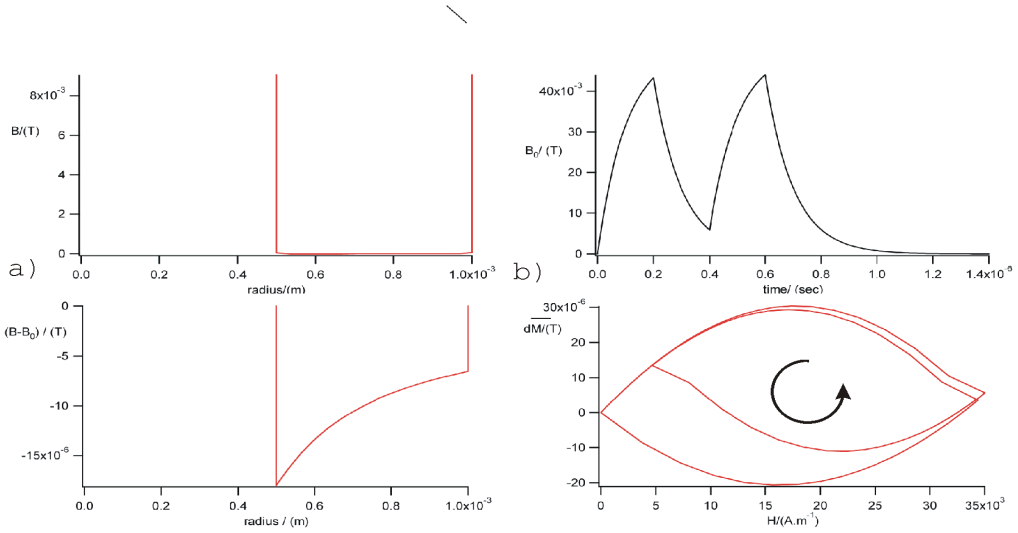

Figure 5:
profile and loss cycle of a ring calculated without self-inductance
a) upper diagram: B-r - profile of the ring shortly after starting up a pulse
lower diagram: $(B - B_S) - r$ - profile
parameter: $\Delta T = 10^{-7}$s, resolution $10p/\Delta T$, 3 equations
b) upper diagram: exciting field B_0 vs. time t
lower diagram: non-stationary loss cycle: $d\bar{M} - H$ - diagram of the ring
parameter: $\Delta T = 10^{-7}$s, resolution $10p/\Delta T$, 3 eqns., heating time for 1°K: ≈ 0.4s

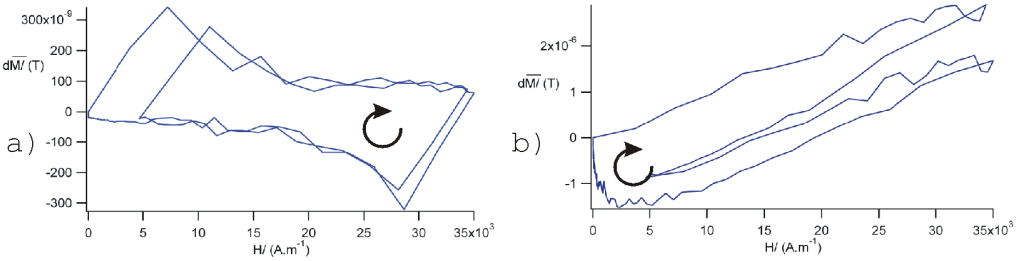

Figure 6:
non-stationary gain cycles of a ring: $d\bar{M} - H$ - cycles with different frequencies:
a) parameter:$\Delta T = 10^{-6}$s,resolution $10p/\Delta T$,4 eqns., cooling time for 1°K: ≈ 59.4s
b) parameter:$\Delta T = 10^{-8}$s,resolution $10p/\Delta T$,4 eqns., cooling time for 1°K: ≈ 0.19s
diagram B_0 vs. time t as in Fig.5b) but time baseline for a) x10, for b) :10

Effective "cooling down" a superconductor by microwaves is a known effect [9], but is attributed to a lowering of T_C and the gap energy. Here it is explained as real temperature decrease. The effect seems to be generated by self induction.
We compare the theory with prior work:
The term d^2B/dt^2, the consideration of flux and the self induction is not present in all prior versions [15] - [17]. They are more simple and better suited for the application of analytic solution methods.
Furthermore, our result of τ differs to ref. [17]:
We find $\tau = (m\sigma)/(n_R q^2) = 4,7694.10^{-8}$ sec.
From [17] it follows $\tau = 4\pi\sigma\lambda_L^2/c^2 = (m_S\sigma)/(n_S q_S^2) = 0,53375.10^{-10}$ sec
(Here $\lambda_L^2 = m_S c^2/(4\pi n_S q_S)$ is in cgs-units, cf. [8].)
The cause of this difference is the separate handling of resistive and superconductive charges in this article.

5 Outlook

If the theory can be evaluated by experiments it will be transferred to high-T_c-superconductors. This will show its technological relevance.

6 Appendix: - the implementation of the code

The material data of lead necessary for the program are shown in Tab.1.
The differential equation system has to be rewritten as a system of first order.
We redefine $y_1 := B(r)$, $y_2 := y_1' := dB/dr$, $y_3' := d\Phi/dr$, $y_4' := d\phi/dr$, $y_5 := B - B_S$ and $y_6 := d(B - B_S)/dr$ and obtain (cf. eq.[19] - [22])

$$\begin{pmatrix} y_1' \\ y_2' \\ y_3' \\ y_4' \\ y_5' \\ y_6' \end{pmatrix} = \begin{pmatrix} y_2 \\ y_1/\lambda_L^2 - y_2/r + d^2B/dt2 - 2\mu_0 q n_R v_m/r^2 \\ ry_1 + \mu_0 q n_R y_4 \\ v_m \\ y_6 \\ y_5/\lambda_L^2 - y_6/r + d^2B/dt2 - 2\mu_0 q n_R v_m/r^2 \end{pmatrix} \tag{30}$$

This is the most complex version to tackle the problem. The differential equations can be solved by the MATLAB routines **bvp4c** or **bvp5c**. In the beginning the solving functions are given as estimating functions on the interval. At the chosen x-coordinates the points are calculated and interconnected by spline functions in the program. A Least-Square routine minimizes

Table 1: material data of Pb

		value	**units**	**ref.**
T_C	critical temperature	7,193	K	[8]
λ_0	penetration depth ($T = 0$)	$3,7.10^{-8}$	m	[8]
λ_L	penetration depth at T	$\lambda_L = \lambda_0/\sqrt{1-(T/T_C)^4}$	m	[9]
n_S	supercond. electron density	$m_S/(\lambda_L^2 \mu_0 q_S^2)$	m^{-3}	[8]
N_F	density of electrons $< \epsilon_F$	$13,2.10^{28}$	m^{-3}	[8]
T_F	Fermi temperature	$10,87.10^4$	K	[8]
v	valence bond number	4	-	[8]
n_R	resistive electron density	vN_FT/T_F	m^{-3}	[8]
ρ_{273}	specific resistivity at 273 K	$19,2.10^{-6}$	$\Omega.cm$	[11]
ρ	specific resistivity at 4.2 K	$1,9.10^{-4}\rho_{273}/100$	$\Omega.m$	[11]
σ	specific conductivity	$1/\rho$	$(\Omega.m)^{-1}$	-
T_D	Debye temperature	96,3	K	[12]
c_1	fit coefficient of spec. heat	464,4	$cal.mol^{-1}.K^{-1}$	[12]
c_2	fit coefficient of spec. heat	$7,64.10^{-4}$	$cal.mol^{-1}.K^{-2}$	[12]
M_{Pb}	molecular mass	207,2	$g.mol^{-1}$	[13]
d_{Pb}	mass density	11,35	$g.cm^{-3}$	[14]
C_P	spec.heat per mol	$c_1(T/T_D)^3 + c_2T$	$cal.mol^{-1}.K^{-1}$	[12]
C_{P_Vol}	spec. heat per volume	$4,186.10^3.C_P.M_{Pb}^{-1}.d_{Pb}^{-1}$	$J(dm^{-3}K^{-}1)$	-

the summed squared deviations from the differential equation $F(y_i, \dot{y}_i) = 0$. The iteration yields the radial profile $B(r)$ of the probe.
The time-dependent algorithm calculates the homogeneous outer magnetic field $B_0(t)$ at every time t_i. This determines the boundary conditions which allow to solve the differential equations of the radial profile at t_i.
Derivatives in the code like $d\Phi/dt(r, t_i)$ are programmed by a difference quotient remembering data solved at the last point at t_{i-1}. Similarly d^2B/dt^2 is calculated as a 2-fold difference quotient.

Numeric inputs:
The exponential time constant of the exciting $B_0(t)$ is ΔT,
the time length of the rising or falling slope is $2\Delta T$, in the end $4\Delta T$.
The boundary conditions of a cylinder on an interval $[x_0, r_0]$ are:
y-coordinates: left border:
$y_2 = 0; y_3 = 0; y_4 = 0; y_5 = 0;$

y-coordinates: right border:
$y_1 = B_0(t_i); y_6 = 0;$
r-coordinate: left border $x_0 = 0,00001$; right border $r_0 = 0,001$.
Remark:
$x_0 = 0$ can not be applied due to numerical problems of the solving routine. So, by tolerating a small error, the point x_0 is chosen near to zero .

The boundary conditions of a ring on an interval $[x_0, r_0]$ are:
y-coordinates: left border:
$y_1 = B_0(t_i); y_3 = x_0^2 B_0(t_i); y_4 = 0; y_5 = 0;$
y-coordinates: right border:
$y_1 = B_0(t_i); y_5 = 0;$
r-coordinate: left border $x_0 = 0,0005$; right border $r_0 = 0,001$.
Explanation for y_3 at the left border:
the magnetic field on the left of x_0 is $B = B_0(t_i) + B_i$: The additional field B_i is generated by the superconducting ring currents $\mathbf{j_S} = \mu_0^{-1}\mathbf{rotB}$ close to the right side of x_0. These ring currents have the opposite direction to the ring currents close to the left of r_0. The ring currents at r_0 generate the magnetization $M \approx -B_0$ in the superconductor. At x_0 this influence is canceled, i.e. $M(x_0) = -B_0 - B_i = 0$.
It is possible to regard this setup as two concentric coils: The outer coil at r_0 generates magnetization, the inner at x_0 compensates it. Therefore the field in the inner hollow core is $B = B_0 + B_i \approx 2B_0$. Then, the net flux $y_(x_0) \approx 2.B_0.x_0^2/2$ is the boundary value.

References

[1] Muschik W., Irreversibility and Second Law, J. Non-Equlib. Thermodyn. 23 (1998) 87

[2] Aharoni A., Exchange anisotropy in films, and the problem of inverted hysteresis loop, Journ. Appl. Phys. 76 (1994) 6977

[3] Bauer W. -D., About Energy Conservation, Second Law and Overunity, WDB Verlag, Berlin 2015
see the corrected version at
https://www.overunity-theory.de/Buch_gedruckt_korrigiert.pdf

[4] Santhanam P, Dodds J. O., Ram R.J, Thermoelectrically Pumped Light-Emitting Diodes Operating above Unity Efficiency, Phys. Rev. Lettr. 108 (2012) 097403

[5] Marent A., Entwicklung einer neuartigen Quantenpunkt-Speicherzelle, PhD-Thesis, TU Berlin, 2011

[6] Ye Z. et al., Phonon-assisted up-conversion photoluminescence of quantum dots, Nature communications 12 (2021) 4283

[7] London F. , London H., The Electromagnetic Equations of the Superconductor, Proceedings of the Royal Society A Mathematical, Physical and Engineering Sciences. 149 (866): (1935), 71.

[8] Kittel C., Einführung in Festkörperphysik 4.Auflage,
R. Oldenbourg Verlag München, Wien, 1976

[9] Tinkham M., Introduction to Superconductivity, McGraw-Hill, New York, 1996

[10] Bronstein I., Semendjajew K,, Taschenbuch der Mathematik, Verlag Harri Deutsch, Thun, Frankfurt, 1983

[11] Jensen J.E., Tuttle W.A., Stewart R.B., Brechna H., Prodell A.G., Editors, Cryogenic Data Handbook, BNL 10200-R, Revised August 1980
see http://wpw.bnl.gov/rgupta/cryogenic_data_subject/section10.pdf

[12] Horwitz M., Silvidi A.A, Malaker S.F. , Daunt J.G., Phys.Rev. 88 (1952) p.1182

[13] Wedler G;, Lehrbuch der physikalischen Chemie 4.Auflage, Wiley-VCH, Weinheim, 1982

[14] https://www.wikipedia.org

[15] M. W. Coffey and J. R. Clem, Phys. Rev. B 46, 11757 (1992)

[16] Kopnin N. B. , Theory of Nonequilibrium Superconductivity Oxford University Press, New York, 2001

[17] Kogan V.G., Phys. Rev. B 97, 094510 (2018)

[18] Amon A., Lefranc M., Nonlinear Dynamics, De Gruyter, Berlin, 2023